The International Journal of Advanced Manufacturing Technology (2018) 99:1109–1117
https://doi.org/10.1007/s00170-018-2513-9

ORIGINAL ARTICLE

Evaluation of grinding wheel loading phenomena by using acoustic emission signals

Chien-Sheng Liu[1] · Yu-An Li[2]

Received: 18 April 2018 / Accepted: 24 July 2018 / Published online: 16 August 2018

Abstract
In the industrial manufacturing field, machining is a major process. Machining operations involve grinding, drilling, milling, turning, pressing, molding, and so on. Among these operations, grinding is the most precise and complicated process. The surface condition of the grinding wheel plays an important role in grinding performance, and the identification of grinding wheel loading phenomena during the grinding process is critical. Accordingly, this present study describes a measurement method based on the acoustic emission (AE) technique to characterize the loading phenomena of a Si_2O_3 grinding wheel for the grinding mass production process. The proposed measurement method combines the process-integrated measurement of AE signals, offline digital image processing, and surface roughness measurement of the ground workpieces for the evaluation of grinding wheel loading phenomena. The experimental results show that the proposed measurement method provides a quantitative index from the AE signals to evaluate the grinding wheel loading phenomena online for the grinding mass production process, and this quantitative index is determined via some experiments in advance in the same grinding environment to help the monitoring and controlling of the grinding process.

Keywords Acoustic emission (AE) · Surface grinding · Process monitoring · Grinding · Wheel loading · Surface roughness

1 Introduction

In addition to the flourishing of the modern manufacturing industry, product precision requirements are becoming increasingly stringent. In the industrial manufacturing field, machining is a major process. Machining operations involve grinding, drilling, milling, turning, pressing, molding, and so on. Among these operations, grinding is the most precise and complicated process. The surface condition of the grinding wheel plays an important role in the grinding performance because the condition of the grains on the periphery of the grinding wheel has a major influence on the damage induced in a ground workpiece [1]. Grinding wheel loading means detached chip accumulation in porous spaces between abrasive grains of the grinding wheel. This phenomenon produces dull wheel grains that lead to deteriorating wheel cutting ability and results in excessive rubbing and vibration [2–4]; it also reduces the life of the grinding wheel and increases the grinding force and temperature [5]. As a result, the identification of grinding wheel loading phenomena during the grinding process is critical and necessary. Because grinding is a complicated process, it is necessary to develop a reliable online monitoring technique to supervise the process [6]. In the literature, various monitoring techniques have been used for the online characterization of grinding processes. Among them, the acoustic emission (AE) technique is generally thought to be the most efficient and sensitive process [6–8]. The AE wave is a type of non-stationary stochastic signal. AE signals provide a variety of information regarding the grinding process. However, stricter analyses may be obtained by processing these signals with the help of statistical parameters to obtain information that can correlate the signals with the phenomena under study. Among the available statistics for manufacturing monitoring based on the AE signal, the root mean square (RMS) value of the AE signal

✉ Chien-Sheng Liu
csliu@mail.ncku.edu.tw

[1] Department of Mechanical Engineering, National Cheng Kung University, No. 1, University Road, Tainan City 70101, Taiwan

[2] Department of Mechanical Engineering and Advanced Institute of Manufacturing with High-tech Innovations, National Chung Cheng University, No. 168, University Road, Minhsiung Township, Chiayi County 62102, Taiwan

(AE_{RMS}) is the most used. The AE_{RMS} can be expressed as follows:

$$AE_{RMS} = \sqrt{\frac{1}{\Delta T}\int_0^{\Delta T} AE_V{}^2(t)dt}, \quad (1)$$

where $\triangle T$ is the integration time constant, and AE_V is the instantaneous signal [9, 10].

The fast Fourier transform (FFT) is often used for extracting the features of AE signals in the frequency domain. However, AE in the grinding process is the transient elastic energy spontaneously released when materials undergo deformation, fracture, or both. For these non-stationary transient signals, the FFT presents only the average values of the frequency components over the duration of its sampled span. As a result, the FFT cannot adequately describe the characteristics of the transient signals in both the time and frequency domains [11].

The AE technique during grinding can offer much real-time sensory information, such as tool condition, machine dynamics, and workpiece quality [12–21]. For example, Dornfeld et al. used AE sensing technology and other sensors to monitor and analyze grinding wheel loading phenomena and first discussed the relationship between the AE signal and the grinding force [22]. Yossifon et al. investigated the characteristics of grinding wheel wear caused by the grinding of workpiece materials with high adhesion, as these adhesive materials are prone to wear and generate heat from grinding. Loading phenomena, which shorten the lifetime of the grinding wheel, can also occur. A comparative analysis of the grinding force and amount of loading has been analyzed; the trend of their curves was found to be rather similar [23–25].

Traditionally, the monitoring task of the grinding wheel loading is usually conducted by the operator. To achieve full automation of machining operations, there has been an earnest interest in developing automated monitoring technologies for grinding wheel loading phenomena [8]. Surface integrity is closely related to both the grinding force and the temperature in the grinding process, and the grinding wheel surface plays an important role in the surface roughness of the ground workpieces [26, 27]. However, to the best of our knowledge, grinding is complicated, and it is difficult to find a general rule to fit any grinding parameters. In addition, the cost reduction is a very important consideration in the mass production process of the industrial manufacturing field. As a result, in this present study, we propose a practical measurement method to characterize the loading phenomena of a Si_2O_3 grinding wheel using the AE technique for the grinding mass production process. We use a traditional surface-grinding machine tool to investigate the grinding state of the grinding wheel caused by the loading phenomena during the grinding process, and we use a commercial AE sensor as a monitoring device for instantaneous monitoring with low cost. In this manner, we can instantly detect the manufacturing process of the machine and collect the manufacturing signals of the machine through the AE_{RMS} signal of the AE sensor. The proposed measurement method combines the process-integrated measurement of AE signals, offline digital image processing, and surface roughness measurements of the ground workpieces for the evaluation of grinding wheel loading phenomena. By applying a data analysis method, we can effectively and instantly provide a quantitative index for the loading effect and provide early warning to the operator at an appropriate time, thereby allowing the operator to pause the machine, adjust the status of the machine or its parameter settings, and re-start the manufacturing procedure in a grinding mass production process. The remainder of this present study is organized as follows. Section 2 describes the proposed measurement method and experimental procedure. Section 3 discusses the experimental characterization of the proposed measurement method. Finally, Section 4 presents some brief concluding remarks.

2 Proposed methodology and experimental procedure

As shown in Fig. 1, the experiments are performed on a Seedtec YSG 618H surface grinder with a KINIK 93A46H11V Si_2O_3 grinding wheel in this study. For this machine, the rotation speed of the grinding wheel is fixed, and it does not use cutting coolant. A commercial Balance Systems VM25 B512675 AE sensor with a sampling rate of 20 Hz (as shown in the red rectangle) is

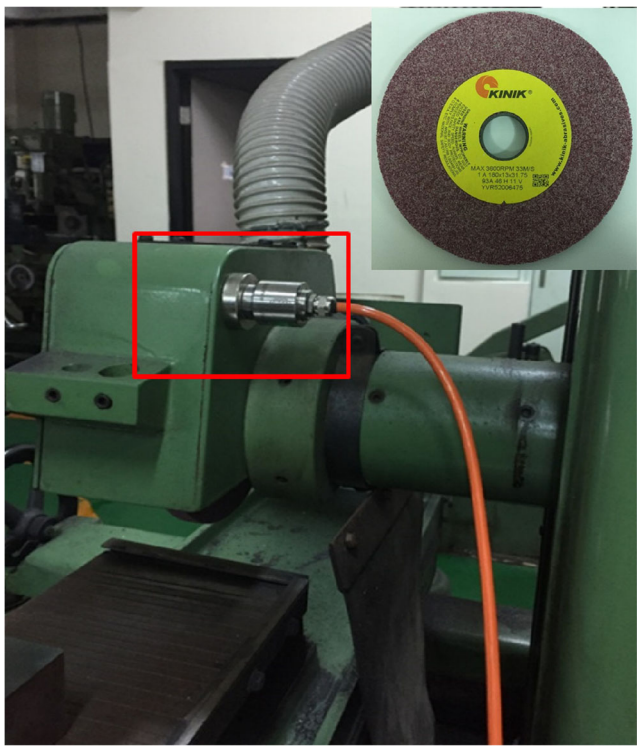

Fig. 1 Photographs of the grinding machine and the grinding wheel

attached to the spindle box surface to pick up the AE signals. Because this sampling rate is far smaller than the frequencies of raw AE signals (≧ 20 kHz), the AE_{RMS} is used for this study. In this study, we investigate grinding wheel loading phenomena under different grinding parameters. These grinding parameters are shown in Table 1. The experimental parameters are selected according to the relevant reference literature and the variable parameters of the machine. The main parameters of normal grinding processing include the rotation speed of the grinding wheel, the type of grinding wheel, the material of the workpiece, the moving velocity of the machine table, the depth of the cut, and the use (or lack of use) of cutting coolant.

Figure 2 presents a flowchart showing the basic steps in the grinding procedure. The proposed measurement method combines the process-integrated measurement of the AE signals, offline digital image processing, and surface roughness measurements of the ground workpieces for evaluation of grinding wheel loading phenomena. The workpiece surface is ground until the loading phenomenon occur, and the trend of the AE signals, measured surface roughness of the workpieces, and measured values of wheel loading over the grinding wheel surface are investigated under different experimental grinding parameters. In this study, the surface roughness R_a of these workpieces is measured using a Mitutoyo SJ-411 surface roughness tester. To determine the loading areas over the grinding wheel surface, a method based on offline digital image processing is used because this method has the advantages of fast processing and low equipment costs [27]. Next, both the measured results for the surface roughness of the workpieces and the values of wheel loading over the grinding wheel surface are compared with the AE signals to evaluate the grinding wheel loading phenomena.

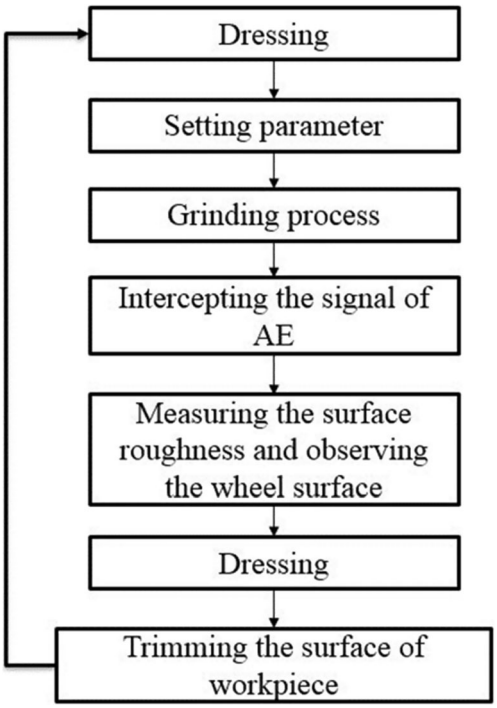

Fig. 2 Flowchart of the grinding procedure

3 Experimental characterization of proposed measurement method

3.1 AE signals

Figure 3 shows the measured AE signals when the grinding depths of the cut are 0.01, 0.015, and 0.02 mm at a table speed of 25.8 m/min, along with the comparison of the results for these three parameters of each of the grinding depths of the cut. Figure 4 shows the measured AE signals when the table speeds are 5.25, 14.6, and 25.8 m/min at grinding cut depths of 0.02 mm. It can be seen from Figs. 3 and 4 that there are three stages of grinding (the early stage, middle stage, and late stage). The early stage of grinding is the first stage when the AE signal rapidly increases. As the number of workpieces that are ground increases, the variation trend in the AE signal also gradually increases. From the comparison of results for the different grinding cut depths (Fig. 3d) and different table speeds (Fig. 4), when the grinding cut depth is relatively deep and when the table speed is relatively fast, the AE signal is relatively large. With the increase in the grinding cut depth and table speed, the deformation of the chip and the friction between grains and workpiece is aggravated, and more grains participate in cutting; as a result, both the grinding force and the AE signal increase [24].

During the middle stage of grinding (second stage), the increasing trend of the AE signal gradually becomes slower because the loading chip on the grinding wheel surface gradually approaches the saturated state, and the relative movement between the grinding wheel and workpieces becomes sliding friction. From the comparison of the experimental results for different grinding cut depths and table speeds (Figs. 3d and 4), there is not a large difference between their AE signals. However, we still observe a phenomenon from the shape of the curves of the AE signals. As shown in Figs. 3d and 4, when the grinding depth of the cut increases and the

Table 1 Grinding parameters of the proposed measurement method

Variable	Corresponding value
Machine	Seedtec YSG 618H
Spindle speed	3450 rpm
Grinding wheel	KINIK 93A46H11V
Workpiece material	A6061
Table speed	5.28, 14.6, 25.8 m/min
Depth of cut	0.01, 0.015, 0.02 mm
Coolant	NA

NA not applicable

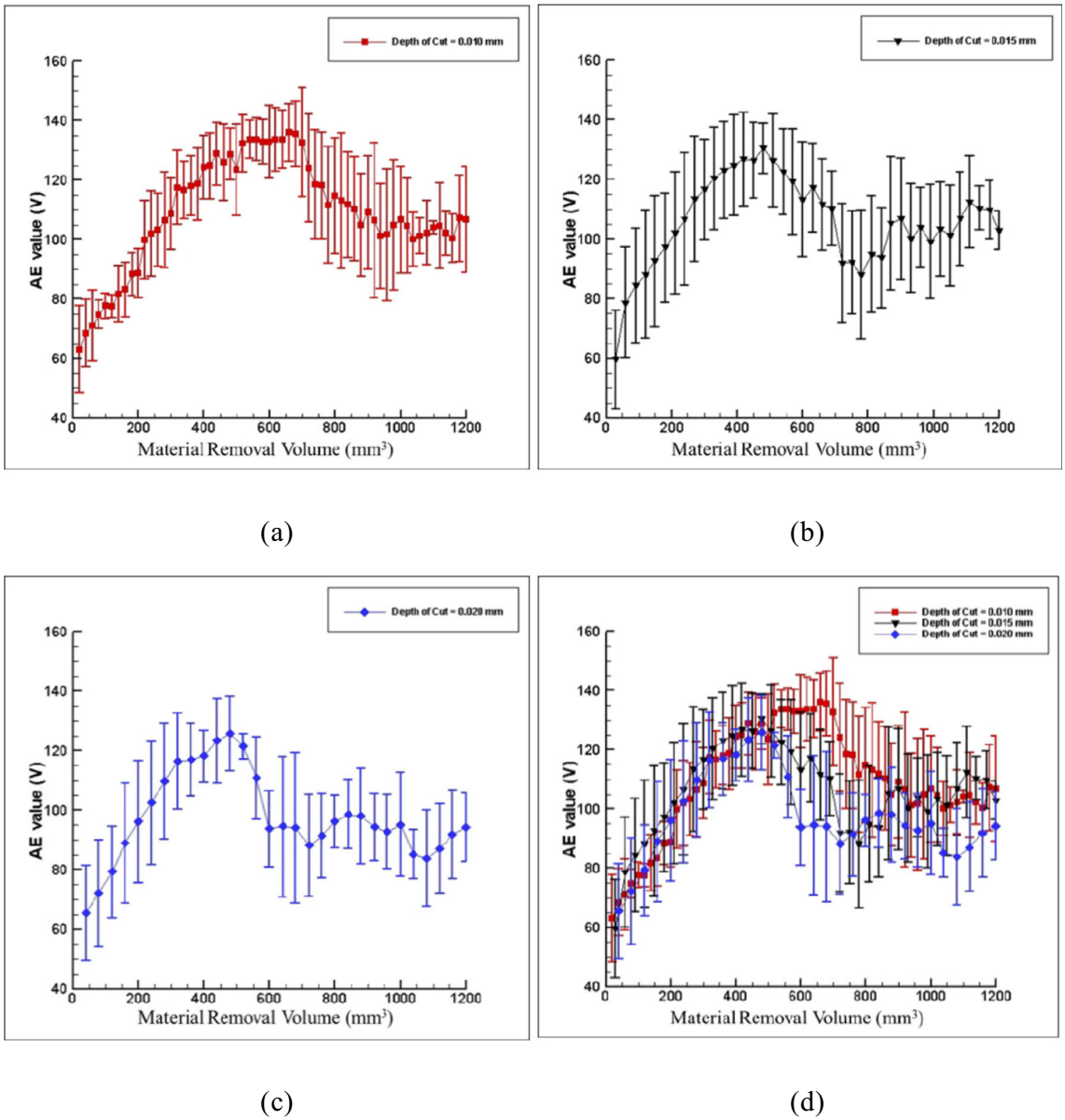

Fig. 3 Measured AE signals when the grinding cut depths are (**a**) 0.01 mm, (**b**) 0.015 mm, (**c**) 0.02 mm, and (**d**) comparison between the AE signals for different grinding cut depths

grinding time becomes shorter, the detached chips more easily accumulate onto the grinding wheel surface. As a result, the amount of wheel loading over the grinding wheel surface rapidly saturates. This phenomenon causes the abrasive grains of the grinding wheel, which cannot bear the excessive grinding force, to fall off during the follow-up grinding, thus producing the AE signals seen during the late stage of grinding.

During the late stage of grinding (final stage), the AE signals can be divided into two sub-stages for the purpose of discussion. During the first sub-stage, the abrasive grains and adhesive of the grinding wheel cannot bear the excessive grinding force; as a result, the loading chips and abrasive grains tend to fall off from the grinding wheel surface. Consequently, cracks form on the original grinding wheel surface, and some abrasive grains adhere to the loading chip and fall onto the workpiece surface during the first sub-stage. With the subsequent grinding proceeding, the grinding burn arises, and chip adhesion becomes severe and can be observed on the workpiece surface (as shown in Fig. 5). As a result, more abrasive grains fall from the grinding wheel, further changing the original morphology of the grinding wheel surface. In the subsequent grinding process, only part of the abrasive grains actually grinds the workpiece surface; therefore, the value of the AE signal gradually declines. In the second sub-stage, when the grinding is continuously operated, the grinding wheel tends to progressively self-sharpen. Figure 6 shows the photograph of the abrasive grains (purple color) that fell from the grinding wheel due to progressive self-

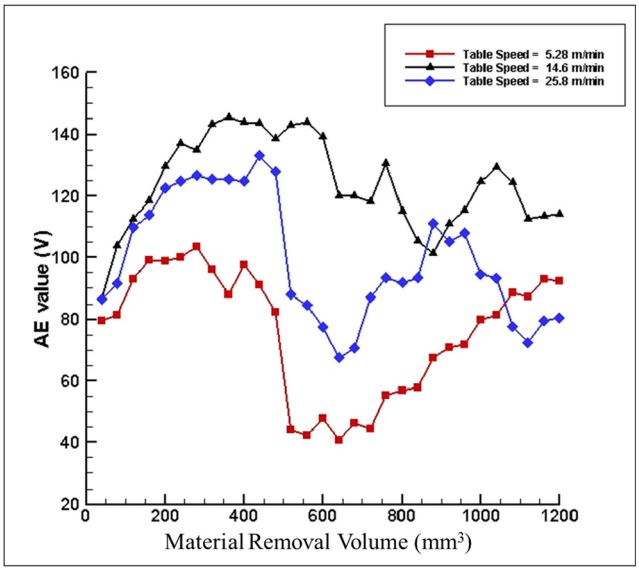

Fig. 4 Measured AE signals with material removal volume for different table speeds

sharpening. Then, the new abrasive grains of the grinding wheel touch the workpiece surface, and the workpiece chips will continue to stick to the pores and the surface of the grinding wheel, producing the loading phenomenon once again. As a result, the AE signal will gradually increase until the grinding wheel surface is loaded, and it again returns to the situation in the first sub-stage, thereby forming a periodic cycle.

3.2 Digital image processing

In this study, an offline digital image processing technique is used to analyze the captured image of the wheel surface and determine the loading areas over the grinding wheel surface. An AM4113T Dino-Lite Premier Digital Microscope is used to capture the image of the wheel surface. The procedure of proposed digital image processing comprises four basic steps, namely, (1) gray processing and histogram equalization, (2) binary processing, (3) overlap processing, and (4) morphology processing.

Fig. 5 Photograph of chip adhesion on the workpiece surface

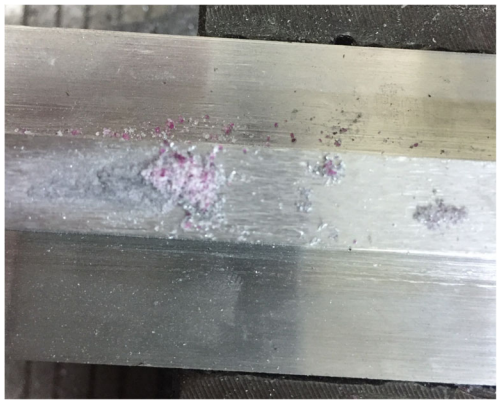

Fig. 6 Photograph of abrasive grains that fell from the grinding wheel

Figures 7 and 8 present the original experimental image on the surface of the grinding wheel and the processed experimental images, showing various processing steps. As shown in Fig. 7, the original captured experimental image is colorful; thus, it is transformed into gray scale image by using gray processing. Here, to increase the contrast of regions of the image, the histogram equalization process is used. Note that Ko et al. (2013) and Adibi et al. (2014) provide a more comprehensive description of the histogram equalization process [27, 28]. Figure 8a presents the processed image following histogram equalization. As shown in Fig. 8a, the metal loading debris is characterized by a high gray level and a high gradient. The metal loading debris can therefore be detected by a simple binary thresholding procedure. During the binary thresholding process, individual pixels in an image are labeled "metal loading debris" if their pixel values are greater than the threshold value; other pixels are labeled "background." In this study, different threshold values are considered to determine the suitable value; however, it is difficult to determine because of the wide range of gray levels of the background (abrasive grains and others). For example, as shown in Fig. 8b, in this case, the threshold value is set at 130, a middle level. From this figure, some abrasive grains are misjudged as metal loading debris. Alternatively, if the threshold value is set at 200, a high level, some metal loading debris is misjudged as background. To overcome this issue, a step of overlap processing is utilized in this study. In this step, many binary images with different threshold values are overlapped into another image, as shown in Fig. 8c. When comparing Fig. 8a, c, it can be observed that the overlap processing increases the contrast of the image. Having done so, another simple binary thresholding procedure followed by a morphological operation is performed to segment the metal loading debris from the image, as shown in Fig. 8d. Figure 9 shows the comparison between another original image and its image processing result. When comparing Figs. 7, 8d and 9, it is obvious that the proposed digital image processing can successfully segment the metal loading debris from the original image and that the proposed digital image processing is reliable.

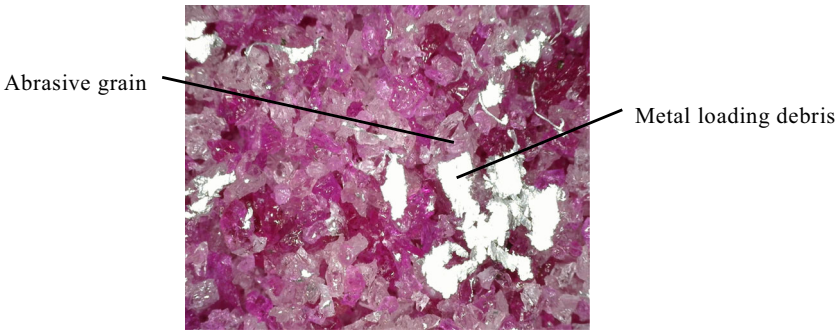

Fig. 7 Original experimental image of the grinding wheel surface

3.3 Wheel loading

The areas of metal loading debris over the grinding wheel surface can be successfully extracted from the original image by using the procedure of proposed digital image processing. Here, MATLAB image processing functions are used. The percentage of the loading amount to the grinding wheel surface can be calculated by dividing the pixel numbers of the metal loading debris by the total pixel numbers of the grinding wheel surface. In this section, the grinding depth of the cut in the grinding parameters is selected as 0.02 mm for comparison purposes. Figure 10 compares the measured AE signals and the measured wheel loading with the material removal volume. As shown, the measured wheel loading is sampled five times, and the average value is taken. It can be observed that both of the curves of the measured AE signals and the measured wheel loading are similar in trend. The loading amount over the grinding wheel surface during the early stage of grinding gradually increases. Although the loading amount during the middle stage of grinding decreases initially, the loading amount is also the greatest when the AE signal is largest. During the late stage, the loading amount gradually decreases to reach a stable variation. According to the experimental results, there is a strong positive correlation between the AE signals and the grinding wheel loading phenomena for the surface-grinding machine tool.

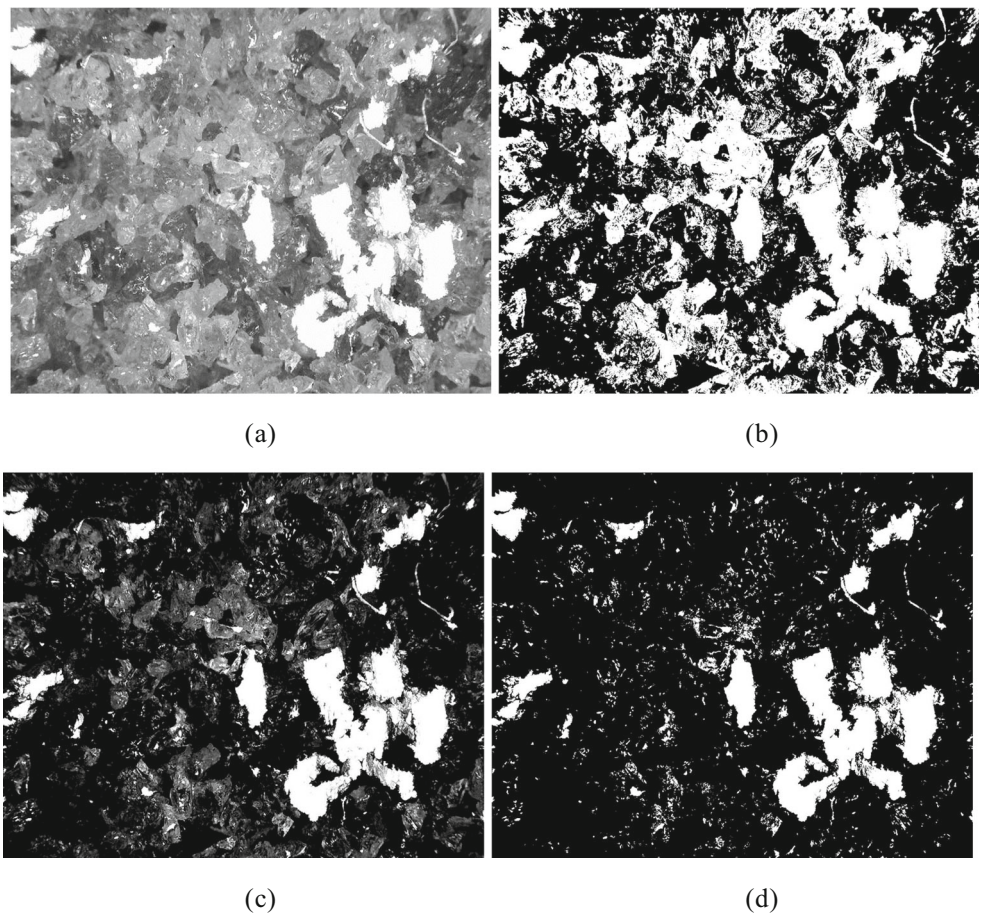

Fig. 8 Image processing results. **a** Gray processing and histogram equalization. **b** binary processing. **c** Overlap processing. **d** Morphology processing

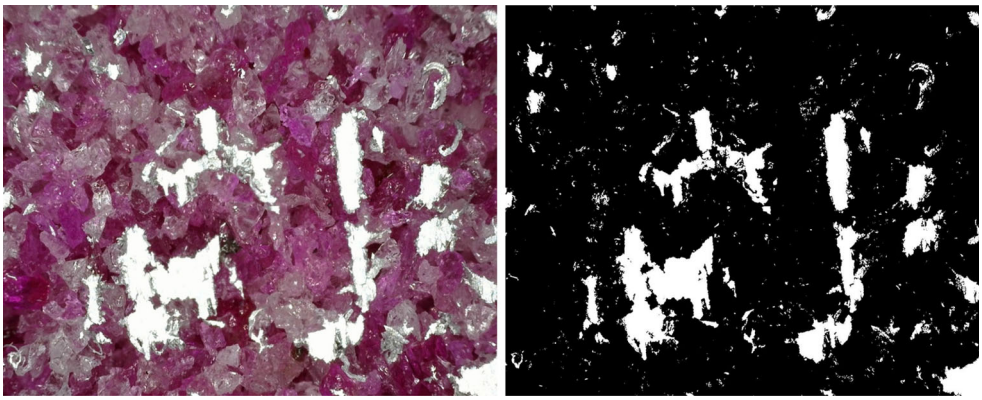

(a) (b)

Fig. 9 **a** Another original experimental image of the grinding wheel surface and **b** its morphology processing result

3.4 Surface roughness

In this section, the grinding depth of the cut in the grinding parameters is also selected as 0.02 mm for comparison purposes. Figures 11 and 12 compare the measured surface roughness R_a as well as the measured AE signals and the measured wheel loading with the material removal volume, respectively. As shown, the measured surface roughness R_a is sampled three times, and the average value is taken. It can be observed that, during the early stage of grinding, R_a also gradually increases (to 1.5 μm). Although R_a during the middle stage of grinding first decreases, R_a is greater than that of the early stage of grinding (to 2 μm) when the AE signal is the largest. During the late stage, R_a gradually increases to reach a stable variation (between 5 and 6 μm) and has an opposite trend when compared to the wheel loading amount.

Three stages of AE signals are identified during the grinding process. During the early stage of grinding, the AE signal rapidly increases, the grinding quality of the workpiece is superior, and the loading amount over the grinding wheel surface gradually increases. During the middle stage of grinding, the grinding quality of the workpiece is at a moderate level, and the loading amount is the greatest. During the late stage of grinding, the grinding quality of the workpiece is the worst, and the loading amount gradually decreases to reach a stable variation. In this study, the AE signal of 110 V (at the end of the early stage of grinding) is a quantitative index to address the grinding wheel.

As a consequence, the experimental results show that the proposed measurement method could provide a quantitative index from the AE signals to evaluate the grinding wheel loading phenomena online at the selected grinding parameters. For the grinding mass production process, because the grinding parameters are fixed, the quantitative index of the AE signal (at the end of the early stage of grinding) could be determined via some experiments in advance in the same

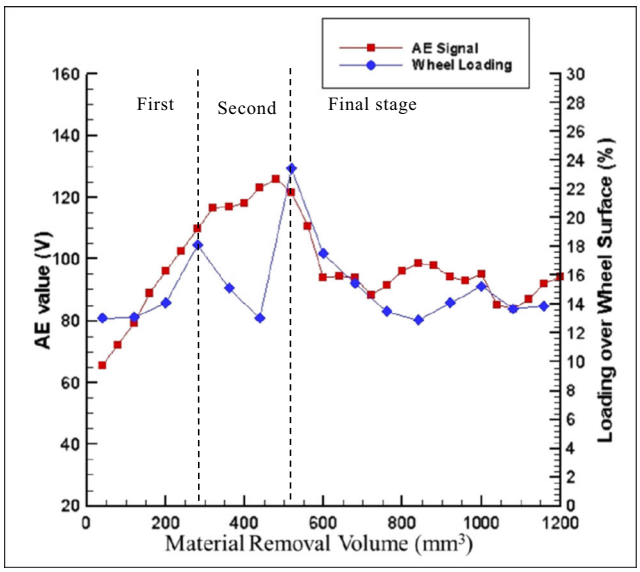

Fig. 10 Comparison of the measured AE signals and the measured wheel loading with material removal volume

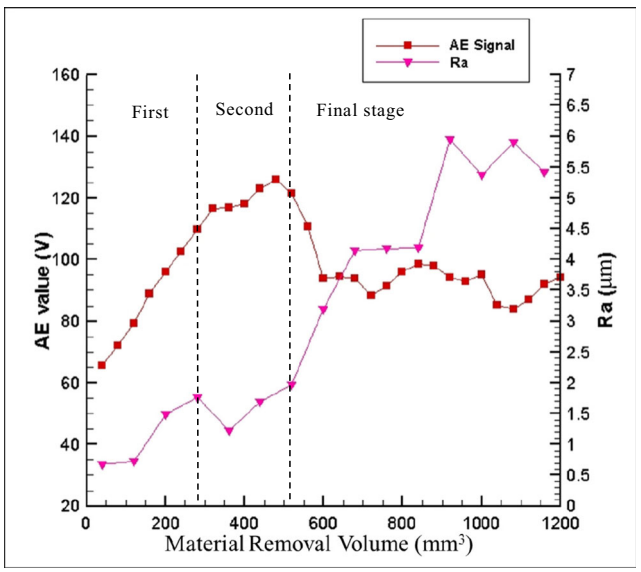

Fig. 11 Comparison of the measured AE signals and the measured surface roughness with material removal volume

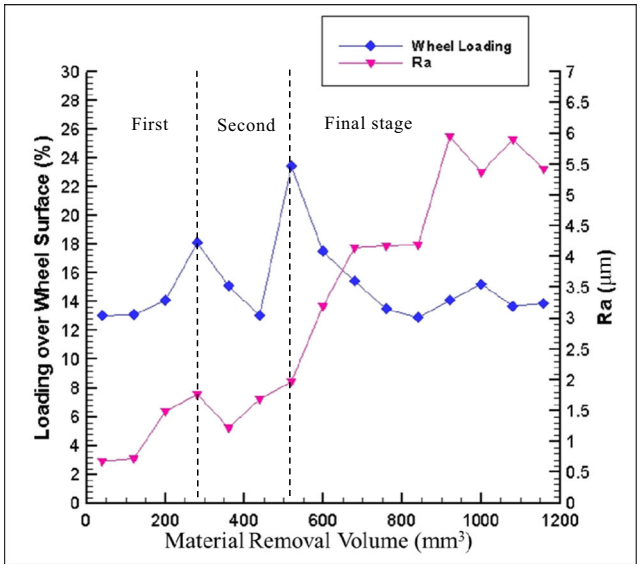

Fig. 12 Comparison of the measured wheel loading and the measured surface roughness with material removal volume

grinding environment to help the monitoring and controlling of the grinding process. However, if we use the AE signals to deduce the wheel loading as an instantaneous monitoring system and repair the behavior of the grinding wheel at any grinding parameters, we must refer to more experimental parameters and factors, including the establishment of a complete database to use the AE signal, to correctly determine the grinding wheel loading phenomena and to more precisely improve the accuracy of an instantaneous monitoring system to achieve its intended purpose. Because grinding is complicated, it is difficult to find a general rule to fit all of the grinding parameters.

4 Conclusions

Because grinding is a complicated process, it is necessary to develop a reliable online monitoring technique to supervise the identification of grinding wheel loading phenomena during the grinding process. In this study, a measurement method that combines the process-integrated measurement of AE signals, offline digital image processing, and surface roughness measurements of the ground workpieces was developed to characterize and evaluate the loading phenomena of a grinding wheel from AE signals. The experimental results showed that the proposed measurement method could provide a quantitative index from the AE signals to evaluate the grinding wheel loading phenomena and address the grinding wheel online for the grinding mass production process.

Funding information Financial support provided to this study is from the Ministry of Science and Technology of Taiwan under Grant Nos. MOST 104-2622-E-194-014-CC2, 106-2622-E-194-004-CC2, and 106-2628-E-194-001-MY3.

References

1. Mokbel AA, Maksoud TMA (2000) Monitoring of the condition of diamond grinding wheels using acoustic emission technique. J Mater Process Technol 101:292–297
2. Adibi H, Rezaei SM, Sarhan AAD (2013) Analytical modeling of grinding wheel loading phenomena. Int J Adv Manuf Technol 68: 473–485
3. Liu Q, Chen X, Gindy N (2007) Assessment of Al_2O_3 and superabrasive wheels in nickel-based alloy grinding. Int J Adv Manuf Technol 33:940–951
4. Cai R, Rowe WB, Morgan MN (2003) The effect of porosity on the grinding performance of vitrified CBN. Key Eng Mater 238:295–300
5. Cameron A, Bauer R, Warkentin A (2010) An investigation of the effects of wheel-cleaning parameters in creep-feed grinding. Int J Mach Tools Manuf 50:126–130
6. Kim HY, Kim SR, Ahn JH, Kim SH (2001) Process monitoring of centerless grinding using acoustic emission. J Mater Process Technol 111:273–278
7. Susič E, Grabec I (2000) Characterization of the grinding process by acoustic emission. Int J Mach Tools Manuf 40:225–238
8. Liao TW, Ting CF, Quc J, Blau PJ (2007) A wavelet-based methodology for grinding wheel condition monitoring. Int J Mach Tools Manuf 47:580–592
9. Martins CHR, Aguiar PR, Frech A, Bianchi EC (2014) Tool condition monitoring of single-point dresser using acoustic emission and neural networks models. IEEE Trans Instrum Meas 63:667–679
10. Liu Q, Chen X, Gindy N (2006) Investigation of acoustic emission signals under a simulative environment of grinding burn. Int J Mach Tools Manuf 46:284–292
11. Li X (2002) A brief review: acoustic emission method for tool wear monitoring during turning. Int J Mach Tools Manuf 42:157–165
12. Sutowski P, Swiecik R (2018) The estimation of machining results and efficiency of the abrasive electro-discharge grinding process of Ti6Al4V titanium alloy using the high-frequency acoustic emission and force signals. Int J Adv Manuf Technol 94:1263–1282
13. Mei YM, Yu ZH, Yang ZS (2017) Experimental investigation of correlation between attrition wear and features of acoustic emission signals in single-grit grinding. Int J Adv Manuf Technol 93:2275–2287
14. Sutowski P, Nadolny K (2017) The identification of abrasive grains in the decohesion process by acoustic emission signal patterns. Int J Adv Manuf Technol 87:437–450
15. Hwang TW, Whitenton EP, Hsu NN, Blessing GV, Evans CJ (2000) Acoustic emission monitoring of high speed grinding of silicon nitride. Ultrasonics 38:614–619
16. Ravindra HV, Srinivasa YG, Krishnamurthy R (1997) Acoustic emission for tool condition monitoring in metal cutting. Wear 212:78–84
17. Susič E, Muzic P, Grabec I (1997) Description of ground surfaces based upon AE analysis by neural network. Ultrasonics 35:547–549
18. Tönshoff HK, Jung M, Männel S, Rietz W (2000) Using acoustic emission signals for monitoring of production processes. Ultrasonics 37:681–686
19. Inasaki I (1998) Application of acoustic emission sensor for monitoring machining processes. Ultrasonics 36:273–281
20. Webster J, Dong WP, Lindsay R (1996) Raw acoustic emission signal analysis of grinding process. CIRP Ann Manuf Technol 45: 335–340
21. Kwak JS, Song JB (2001) Trouble diagnosis of the grinding process by using acoustic emission signals. Int J Mach Tools Manuf 41: 899–913

22. Dornfeld D, Cai HG (1984) An investigation of grinding and wheel loading using acoustic emission. J. Eng. Ind. 106:28–33
23. Yossifon S, Rubenstein C (1981) The grinding of workpieces exhibiting high adhesion. Part 1: mechanisms. J Eng Ind 103: 144–155
24. Yossifon S, Rubenstein C (1981) The grinding of workpieces exhibiting high adhesion. Part 2: forces. J Eng Ind 103:156–164
25. Yossifon S, Rubenstein C (1982) Wheel wear when grinding workpieces exhibiting high adhesion. Int J Mach Tool Des Res 22:159–176
26. Yao C, Wang T, Xiao W, Huang X, Ren J (2014) Experimental study on grinding force and grinding temperature of Aermet 100 steel in surface grinding. J Mater Process Technol 214:2191–2199
27. Adibi H, Rezaei SM, Sarhan AAD (2014) Grinding wheel loading evaluation using digital image processing. J Manuf Sci Eng 136: 011012-1–011012-10
28. Ko S, Liu CS, Lin YC (2013) Optical inspection system with tunable exposure unit for micro-crack detection in solar wafers. Optik 124:4030–4035